

## Effect of local structures on structural evolution during crystallization in undercooled metallic glass-forming liquids

Z. W. Wu, M. Z. Li, W. H. Wang, W. J. Song, and K. X. Liu

Citation: *J. Chem. Phys.* **138**, 074502 (2013); doi: 10.1063/1.4792067

View online: <http://dx.doi.org/10.1063/1.4792067>

View Table of Contents: <http://jcp.aip.org/resource/1/JCPSA6/v138/i7>

Published by the [American Institute of Physics](#).

---

### Additional information on J. Chem. Phys.

Journal Homepage: <http://jcp.aip.org/>

Journal Information: [http://jcp.aip.org/about/about\\_the\\_journal](http://jcp.aip.org/about/about_the_journal)

Top downloads: [http://jcp.aip.org/features/most\\_downloaded](http://jcp.aip.org/features/most_downloaded)

Information for Authors: <http://jcp.aip.org/authors>

### ADVERTISEMENT



**Goodfellow**  
metals • ceramics • polymers • composites  
70,000 products  
450 different materials  
small quantities **fast**

[www.goodfellowusa.com](http://www.goodfellowusa.com)

# Effect of local structures on structural evolution during crystallization in undercooled metallic glass-forming liquids

Z. W. Wu,<sup>1</sup> M. Z. Li,<sup>2,a)</sup> W. H. Wang,<sup>3</sup> W. J. Song,<sup>1</sup> and K. X. Liu<sup>1,b)</sup>

<sup>1</sup>State Key Laboratory of Turbulence and Complex System & Center for Applied Physics and Technology, College of Engineering, Peking University, Beijing 100871, China

<sup>2</sup>Department of Physics, Renmin University of China, Beijing 100872, China

<sup>3</sup>Institute of Physics, Chinese Academy of Sciences, Beijing 100190, China

(Received 15 November 2012; accepted 30 January 2013; published online 19 February 2013)

The effect of local structures on structural evolution during the crystallization of undercooled ZrCu metallic glass-forming liquid was studied via molecular dynamics simulations. It is found that body-centered-cubic (bcc)-like clusters play a key role in structural evolution during crystallization. In contrast to previous speculations, the number of bcc-like crystal nuclei does not change much before the onset of crystallization. Instead, the development of a bcc-like critical nucleus during annealing leads to a strong spatial correlation with other nuclei in its surroundings, forming a crystalline structure template. It is also found that the size distribution of bcc-like nuclei follows a power-law form with an exponential cutoff in the early stage of annealing, but changes to a pure power-law behavior just before the onset of crystallization. This implies that the crystalline structure template has fractal feature and the undercooled liquids evolve to a self-organized critical state before the onset of crystallization, which might trigger the subsequent rapid crystallization. According to the graph theory analysis, it is also found that the observed large scatter of the onset time of crystallization in different liquid samples results from the connectivity of the bcc-like clusters. © 2013 American Institute of Physics. [<http://dx.doi.org/10.1063/1.4792067>]

## I. INTRODUCTION

Crystallization is a ubiquitous and fundamental nonequilibrium phenomenon in materials science.<sup>1</sup> Understanding the mechanism of crystallization of liquids in atomic level has been a great challenge. This becomes much more critical for the development of bulk metallic glasses (BMGs), because intervening crystallization of the liquids in even the most robust BMG-formers is orders of magnitude faster than in many common polymers and silicate glass-forming liquids, thereby significantly influences the glass-forming ability (GFA) and mechanical properties of metallic alloys.<sup>2,3</sup> Figure 1 illustrates the characteristic of the time scale for crystallization and the transformation kinetics from liquid to solid states as a function of temperature, the so-called time-temperature-transformation (TTT) diagram. The shaded undercooled liquid region in Fig. 1 has been considered as a crucial stage for intervening crystallization. So far, some experimental techniques have been developed to suppress the rapid crystallization.<sup>4–7</sup> However, the crystallization rates of these glass-forming metallic liquids are still quite high. Thus, crystallization significantly limits experimental studies of the undercooled metallic glass-forming liquids for a complete understanding of the crystallization mechanism in atomic level.<sup>3,8–10</sup>

On the other hand, some thermodynamical models have been developed for interpreting experimental observations

and understanding the nucleation and growth of crystals in undercooled metallic glass-forming liquids.<sup>8–17</sup> However, these models cannot provide either the direct information of crystallization in atomic level, or the detailed structural evolution in crystallization process. In contrast, molecular dynamics (MD) simulation can provide a deep insight into the atomic mechanism of crystallization of metallic glass-forming liquids. So far, however, little effort has been devoted to it.<sup>16,17</sup> Therefore, it is critical to explore the structural origin of crystallization in undercooled metallic liquids for getting deep insight into the nature of glass formation and developing metallic alloys with excellent GFA.

In this work, we performed classical MD simulations with the LAMMPS package<sup>18</sup> for ZrCu glass-forming alloy and investigated the relationship between local atomic structure and crystallization in undercooled liquid region. The local atomic structures were identified and characterized by Voronoi tessellation, and their time evolution in crystallization process was also analyzed. It is found that the emergence and growth of the critical nucleus formed by the body-centered-cubic (bcc)-like clusters play a key role in the rapid crystallization in undercooled liquid region. The critical nucleus triggers a strong spatial correlation with other crystal nuclei in its surroundings just before the onset of crystallization, which may provide a crystal structure template for the subsequent rapid crystallization. Our further analysis shows that the size distribution of bcc-like nuclei follows a power-law form with exponential cutoff initially, but transforms to a pure power-law behavior, which indicates that there is a significant “chance” for the emergence of a very large bcc-like

<sup>a)</sup>maozhili@ruc.edu.cn.

<sup>b)</sup>kliu@pku.edu.cn.

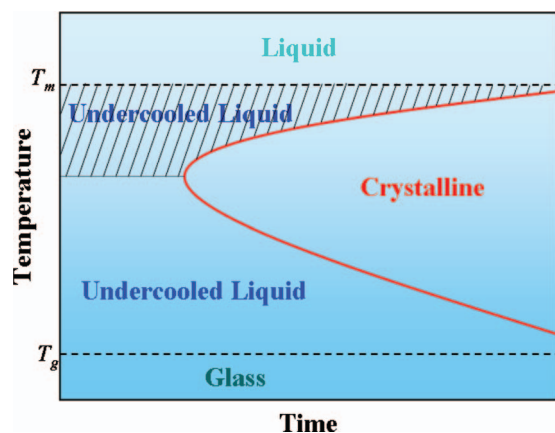


FIG. 1. Schematic of typical time-temperature-transformation diagram for the crystallization of metallic glass-forming alloys. Red curve indicates the onset of crystallization.  $T_m$  and  $T_g$  denote melting and glass transition temperatures, respectively, presented by dashed curves.

nucleus at some time, which triggers the rapid crystallization. In addition, the statistical nature of the critical nucleus formation is found to be closely related to the connectivity of bcc-like clusters in a system.

This paper is organized as follows: in Sec. II, we present our model and method; in Sec. III, results and discussion are given. Finally, a conclusion is presented in Sec. IV.

## II. MODEL AND METHOD

In our MD simulation, the model system of  $Zr_{85}Cu_{15}$  metallic alloy was adopted with a realistic embedded-atom method potential.<sup>19</sup> The structure contains 10 000 atoms in a cubic box with periodic boundary conditions. In the process of sample preparation, it was first melted and equilibrated at  $T = 2000$  K, then cooled down to 300 K with a cooling rate of  $10^{13}$  K/s, during which the cell size was adjusted to give zero pressure in NPT ensemble. The sample was then relaxed for 1 000 000 MD steps at  $T = 300$  K. The MD step is 2 fs. The pair correlation functions (not shown) demonstrate that the simulated sample is in a glassy state.

We first checked the reliability and suitability of the simulated sample by isothermally annealing it and monitoring the evolution of the potential energy at different temperatures of 900, 950, 1000, 1050, 1100, 1150, and 1200 K, respectively. Figure 2 shows the time dependence of potential energy of the sample at different annealing temperatures. It is clearly seen that the potential energy decreases with annealing time at each temperature, but the behavior is quite different. At high temperatures such as 1200 K and 1150 K, the potential energy drops abruptly at a certain time. At low temperatures such as 950 K and 900 K, however, the potential energy drops in a more gradual way. The potential energy drop is the signature of crystallization in the sample, and the different drop behaviors indicate different crystallization rates at different temperatures. The dramatic drop of potential energy in high temperature region also demonstrates that the drastically high crystallization rate indeed limits the experimental studies. On the other hand, the onset time of potential energy drops at different temperatures, as shown in Fig. 2, exhibits

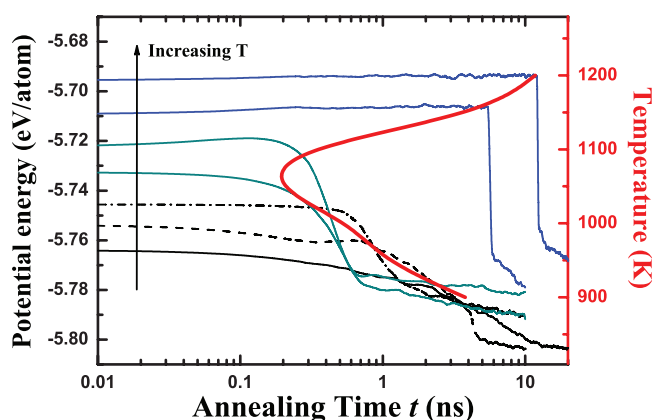


FIG. 2. Time dependence of potential energy of a sample annealed at 900, 950, 1000, 1050, 1100, 1150, and 1200 K (the order is given by the arrow), respectively. The red curve shows the relation between the onset time of potential energy drop and temperature, which exhibits a typical TTT-diagram similar to that in Fig. 1.

a typical TTT-diagram similar to that in Fig. 1 and experimental measurements.<sup>2,5,8</sup> The above results show that the structural model obtained from MD simulations is reliable and suitable for investigating crystallization in undercooled metallic glass-forming liquids. We also checked the size effect on the crystallization behavior. It is found the system size employed in MD simulations is big enough, so that the size effect is negligible.<sup>20</sup>

## III. RESULT AND DISCUSSION

Now we focus on the effect of atomic structures on crystallization in the shaded undercooled liquid region shown in Fig. 1. For the case of  $Zr_{85}Cu_{15}$  metallic alloy,  $T = 1150$  K was chosen for sample annealing. In our studies, five independent samples (denoted as s0, s1, s2, s3, and s4) were prepared and annealed at 1150 K. Figure 3 shows the evolution of potential energy with annealing time in the five independent samples at 1150 K. It is clearly shown that all samples

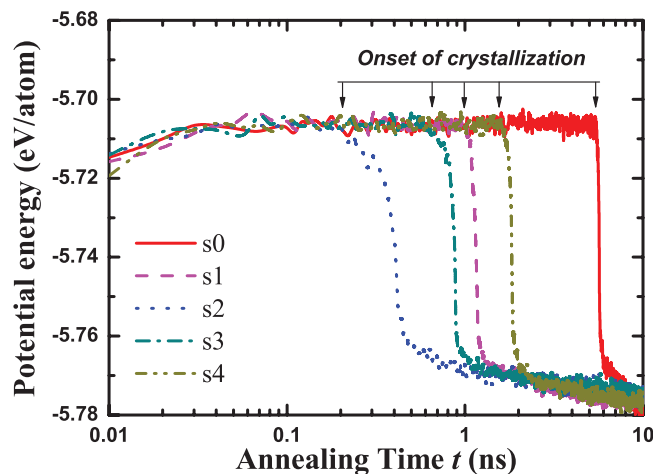


FIG. 3. Time dependence of the potential energies in the five independent samples annealed at 1150 K. The time when potential energy drops is considered as the onset of crystallization.

exhibit rapid crystallization behavior. However, the onset time of crystallization of each sample is quite different. The observation is in good agreement with previous studies.<sup>9,10</sup> The large scatter of the onset of crystallization implies that the crystallization process may rely significantly on the local atomic structures in samples.

### A. BCC-like crystal nuclei

To understand the relationship between the local atomic structures and crystalline nucleation and growth process, we analyzed the detailed structure features for the samples of s0, s1, and s2. The Voronoi tessellation method was employed to characterize the local atomic structures in terms of the Voronoi index  $\langle n_3, n_4, n_5, n_6 \rangle$ , where  $n_i$  represents the number of  $i$ -edged ( $i = 3, 4, 5, 6$ ) faces composing a Voronoi polyhedron,<sup>21–24</sup> so that it may also characterize the atomic symmetry properties for local structures.<sup>25</sup> According to the Voronoi analysis,  $\langle 0,0,12,0 \rangle$  represents icosahedral clusters with five-fold symmetry.  $\langle 0,3,6,4 \rangle$ ,  $\langle 0,3,6,5 \rangle$ ,  $\langle 0,4,4,6 \rangle$ , and  $\langle 0,4,4,7 \rangle$  are considered to be face-centered-cubic (fcc)-like clusters, and  $\langle 0,6,0,8 \rangle$  are bcc-like clusters.<sup>25</sup> During crystallization, the local atomic structures will evolve to fcc- or bcc-crystal-like local configurations. Figure 4(a) shows the evolution of the fraction of fcc- and bcc-like local clusters during annealing. Initially, fcc-like clusters have been already populated in the samples, because of the population of  $\langle 0,3,6,4 \rangle$  in both liquid and glassy states.<sup>23,25</sup> In contrast, the fraction of bcc-like clusters is very small. As the samples are undergoing crystallization, the fraction of both fcc- and bcc-like clusters increases. However, the fraction of bcc-like clusters increases much more dramatically than that of fcc-like ones. The fraction of bcc-like clusters increases more than 40% during the

onset of crystallization. After that, it keeps increasing gradually. For fcc-like clusters, the population increases a little, then decreases gradually, and reaches the initial population values. Thus, the dramatic change of the population of the bcc-like clusters during the onset of crystallization indicates that the bcc-like local atomic structures play a crucial role in the crystallization process in this system.

How do the bcc-like atomic structures influence the crystallization behavior shown in Fig. 3? Next, we will characterize the nuclei formed by the bcc-like clusters in the samples and analyze the nuclei number and size evolution in the crystallization process. To characterize the nuclei formed by bcc-like clusters, we analyzed the connection of the bcc-like clusters based on the graph theory.<sup>26,27</sup> In this scheme, once two bcc-like clusters share at least one common nearest neighbor atom, these two bcc-like clusters are considered to be connected. After checking the connection of all bcc-like clusters, some bcc-like clusters are connected and form a so-called crystal nucleus. Thus, we can identify all the bcc-like crystal nuclei in the samples, and monitor the number and size evolution of these crystal nuclei in the crystallization process. Figure 4(b) shows the evolution of the number of crystal nuclei and the number of atoms in the largest one in the samples of s0, s1, and s2, respectively. It is clear that the number of crystal nuclei is almost the same in these samples and keeps almost constant during annealing. After the onset of crystallization, the number of nuclei decreases quickly. For the largest crystal nucleus, its size is fluctuating before the onset of crystallization. At the onset time of crystallization, the size of the largest nucleus increases drastically, from less than 100 atoms to more than 8000 atoms in a very narrow time window as shown in Fig. 4(b). Meanwhile, a little lag behind fast growth of the largest nucleus, other nuclei are disappearing. This means that as the largest nucleus is growing, the whole system is crystallized rapidly. Therefore, the crystallization in undercooled liquid region is essentially affected by the largest crystal nucleus, but not the number of nuclei. Once the largest nucleus reaches the critical size, its dramatic growth leads to the rapid crystallization. The critical nucleus was estimated to contain about 30~100 atoms, which is similar to the crystal nucleation of colloidal systems.<sup>28,29</sup> The growth rate of the largest crystal nucleus is estimated to be about 25 000 ~ 30 000 atoms/ns.

Previous studies have indicated that the rapid crystallization in undercooled liquid region requires either a fast growth mechanism or a sudden dramatic increase in the nucleation rate.<sup>10</sup> The latter scenario has been used to explain the experimental data, and a good agreement has been obtained, which suggests that the multiple nucleation mechanism may be responsible for the rapid crystallization in shallow undercooled liquid region.<sup>10</sup> However, the multiple nucleation or a sudden dramatic increase in the nucleation rate was not observed in our simulation of crystallization. As shown in Fig. 4(b), the number of the bcc-like crystal nuclei is almost not changing before the onset of crystallization. Our results indicate that in undercooled liquid region the nuclei form following the classical steady state nucleation mechanism.<sup>9–11</sup> Therefore, the rapid crystallization is not triggered by a sudden dramatic increase of nucleation rate, but the fast growth of the largest

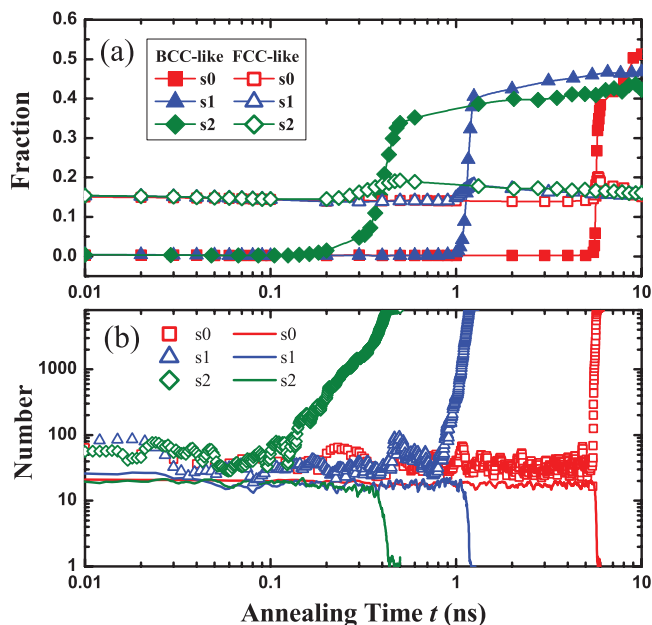


FIG. 4. (a) The change in fraction of fcc- (open symbols) and bcc-like (solid symbols) atoms with annealing time. (b) Number of bcc-like crystal nuclei (solid curves) and number of atoms in the largest nucleus (scattered curves) as a function of annealing time.



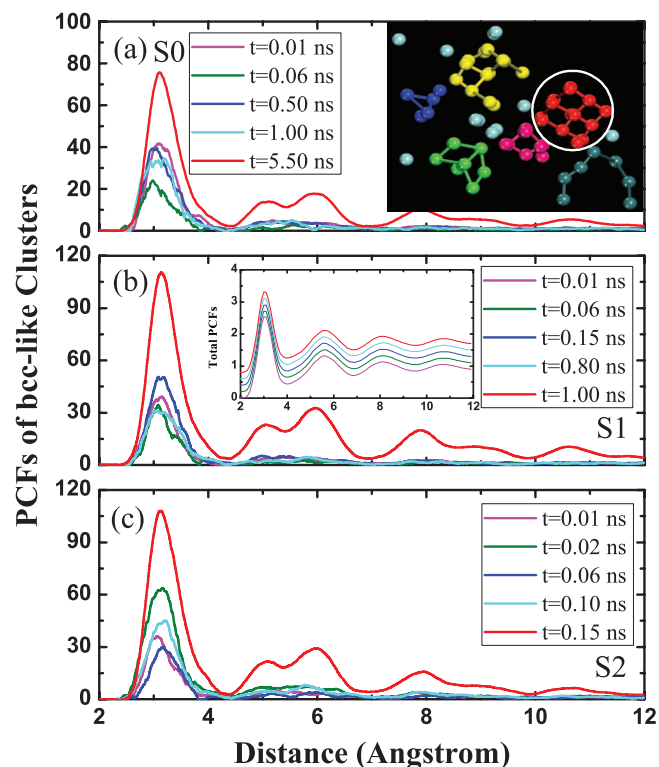


FIG. 5. The pair correlation functions of bcc-like atoms in three samples at different time  $t$  before onset of crystallization. The PCFs were obtained by averaging over 40 structure configurations of  $t \pm 0.004$  ns. The inset in (a) shows the structure configurations of the largest bcc-like crystal nucleus (circled) and the nuclei in its surroundings at  $t = 5.5$  ns in s0. The inset in (b) shows the total PCFs at different time  $t$  in sample s1. The total PCFs in sample s0 and s2 (not shown) are similar to that in s1.

bcc-like crystal nucleus. As shown in Fig. 4(b), as the size of the largest nucleus exceeds the critical size, the rapid crystallization occurs.

## B. Spatial correlation of BCC-like clusters

To get deeper insight into the rapid crystallization facilitated by the fast growth of the critical nucleus, we analyzed the pair correlation function (PCF) for the bcc-like clusters at different annealing times in three samples as shown in Fig. 5. It is found that the PCF of bcc-like clusters in the nearest-neighbor distance exhibits significant fluctuation before the onset of crystallization in all three samples. However, as the largest bcc-like crystal nucleus reaches the critical size, a strong spatial correlation of the bcc-like clusters is emerging. The spatial correlation extends even beyond 10 Å, in the so-called medium range. The emergence of the strong spatial correlation does not result from the increase of bcc-like clusters, because the fraction of bcc-like clusters is almost unchanging before the onset of crystallization as shown in Fig. 4(a). We also calculated the PCFs of the whole system at different times for each sample. However, it does not exhibit strong spatial correlation as shown in inset of Fig. 5(b). Therefore, the strong spatial correlation of bcc-like clusters may be closely correlated to the rapid crystallization.

Next, we examined the spatial configuration of the largest crystal nucleus and other nuclei in its surroundings at

$t = 5.5$  ns (before the onset time of crystallization) in sample s0 as shown in the inset in Fig. 5(a). Several crystal nuclei were observed to surround the largest nucleus (circled) with almost the same orientation. This was not observed at other times. The largest nucleus together with others in its surroundings might form a crystal structure template in a medium range. As a critical bcc-like crystal nucleus is forming, it may trigger the development of some other nuclei in its surroundings, as demonstrated in the inset in Fig. 5(a). The strong spatial correlation of bcc-like clusters results in the formation of a structure template, which may be more favorable for the formation of long-range translational order and leads to the subsequent rapid crystallization. The formation of such a structure template might be facilitated by the high mobile atoms in high-temperature samples. As the bcc-like critical nucleus is developing, the mobile atoms in the surrounding may facilitate its structural information even up to the medium range, leading to the strong spatial ordering and the formation of the medium-range crystal structure template. In the low temperature region, however, atoms are much less mobile and the atomic rearrangement is quite slow, so that such a spatial correlation of bcc-like clusters cannot be formed as quickly as that in high temperature region. Therefore, although a high nuclei density was observed in experiments in low temperature region,<sup>8</sup> the crystallization process is much more slowly as shown in Fig. 2.

## C. Size distribution of BCC-like nuclei

It is interesting to investigate the size distribution of the bcc-like crystal nuclei in the process of crystallization, which may provide more structural information for better understanding the crystallization mechanism. Based on the graph theory analysis, Fig. 6 shows the size distribution of bcc-like nuclei at different annealing times ( $t = 0.06, 0.50, 1.00$ , and

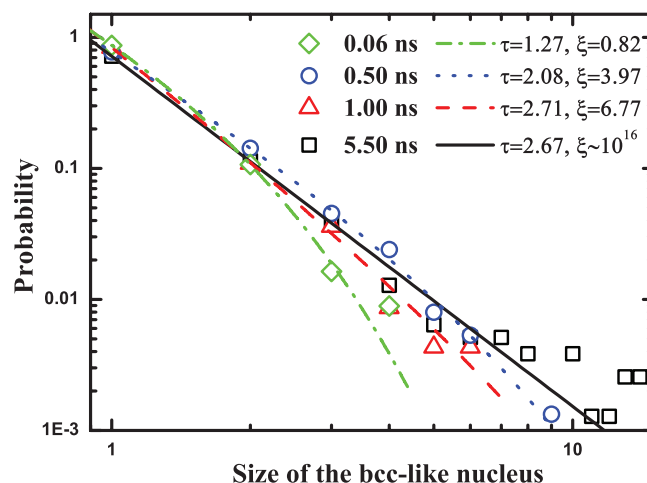


FIG. 6. The size distributions of the bcc-like nuclei in sample s0 at different annealing time  $t$ . The data were obtained by averaging over 40 structure configurations of  $t \pm 0.004$  ns. Note that the size of a nucleus is defined as the number of central atoms of bcc-like Voronoi polyhedra (0,6,0,8). The solid curves were obtained by fitting the data to Eq. (1). The parameters  $\tau$  and  $\xi$  are also presented in this figure.

5.50 ns) for sample s0. The size distribution roughly follows a power-law behavior. However, our data fitting shows that the simulated data do not follow a power-law form perfectly. To get deeper insight into the behavior of the size distribution, we fitted the data by using a power-law form with an exponential cutoff,<sup>26</sup>

$$P(s) \sim s^{-\tau} e^{-s/\xi}, \quad (1)$$

where the fitting parameters  $\tau$  and  $\xi$  represent power-law exponent and cutoff size, respectively. The solid curves in Fig. 6 are obtained by fitting the simulation data to Eq. (1). The value of  $R^2$  is better than 0.999, indicating that an excellent fitting was obtained.

In Eq. (1),  $\xi$  represents a characteristic size of clusters. Here, a finite value of  $\xi$  indicates that there exists a characteristic size of bcc-like nuclei in a system. As shown in Fig. 6,  $\xi$  varies considerably with annealing time. It becomes larger and larger in the process of annealing. Just before the onset of rapid crystallization, the value of  $\xi$  increases dramatically to  $\sim 10^{16}$ . The drastic increase of  $\xi$  suggests the lack of a typical length scale of the bcc-like nuclei, which is the characteristic of self-organized critical behavior.<sup>30–32</sup> On the other hand, as  $\xi$  is getting infinite, the exponential term in Eq. (1) becomes trivial and the size distribution of nuclei follows an “exact” power-law behavior, which is the characteristic of self-organized fractal structure. In addition, the large scatter of the onset time of crystallization observed in both experiments and simulations<sup>5,10</sup> may also imply that there is no a typical time scale for the onset of crystallization. All these indicate that the dynamics of supercooled liquids will eventually evolve to a self-organized critical state spatiotemporally. The power-law size distribution of nuclei at the time just before the onset of crystallization also indicates that there is a considerable “chance” for the emergence of a very large bcc-like crystal nucleus at some time in a sample. Once this event takes place, rapid crystallization occurs.

The variation of the value  $\tau$  is also noteworthy. It characterizes the structure geometry information of a system and is closely correlated to the dimensionality. As shown in Fig. 6, it increases from  $\tau \approx 1.27 (< 2)$  to  $\tau \approx 2.67 (> 2)$ . Previous studies show that  $\tau = 2$  is a dividing line between two fundamentally different behaviors of the complex system.<sup>26</sup> As  $\tau < 2$ , the average properties of the system are dominated by the few bcc-like nuclei with large sizes, whereas systems with  $\tau > 2$  are dominated by those with small sizes. Thus, this will strongly influence the dynamic process of the system. In our simulated samples,  $\tau$  becomes bigger than 2 as the systems evolve to a self-organized critical state, and every nucleus plays an important role in the dynamical process of crystallization. The self-organized critical feature finally triggers a rapid phase transition process. On the other hand,  $\tau$  also characterizes some structure geometry information of a system. In this sense, it may be closely correlated to the dimensionality of the system. Here, we analyzed the dimensionality of sample s0 by using the correlation function  $h(r) \sim r^{-(D-D_f)} \exp(r/r_c)$  proposed in Refs. 33 and 34 and fitting the peaks of the function  $g(r) - 1$  ( $g(r)$  is the PCF of s0

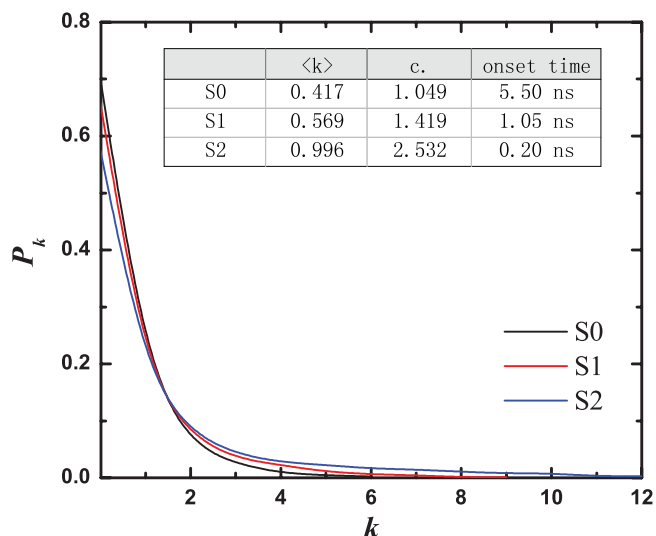


FIG. 7. Probability distribution of degree of bcc-like clusters in three samples. The inset table shows the average value of connectivity  $c$  and degree  $\langle k \rangle$  of bcc-like clusters and the onset time of crystallization.

shown in Fig. 5(a) at  $t = 5.50$  ns,  $5 \text{ \AA} < r < 25 \text{ \AA}$ ). Finally, an excellent fitting was obtained with the fractal dimension  $D_f = 2.74$ , which is very close to the value of  $\tau = 2.67$ .

## D. Connectivity of BCC-like clusters

To understand the observed large scatter of the onset time of crystallization, we analyzed the connectivity of the bcc-like clusters in three samples in terms of graph theory. According to the graph theory, a bcc-like cluster can be considered as a node, so that the degree of a cluster node  $k$  can be defined as the number of adjacent bcc-like clusters by sharing the nearest neighbor atoms. Figure 7 shows the probability distribution function  $P(k)$  of degree of bcc-like clusters. It can be seen that the distribution in s2 extends to bigger  $k$  than those in s0 and s1, which indicates that the bcc-like clusters are connected more tightly in s2. We also investigated the connectivity of bcc-like clusters in a sample defined as  $c = \sum_i w_i / n$ , where  $w_i$  is the number of shared atoms by the bcc-like clusters in the  $i$ th crystal nucleus, and  $n$  is the total number of bcc-like clusters in the sample. It is found that the calculated connectivity exhibits large fluctuation during annealing in all samples. This is because of the effect of relatively high temperatures. If one examines the average value of  $c$  over the time before the onset of crystallization, they (as well as  $\langle k \rangle$ ) show a clear correlation with the onset time of crystallization in three samples, as shown in the table in Fig. 7. The larger the value of  $c$  or  $\langle k \rangle$ , the more tightly and compact the bcc-like clusters are connected with each other, and the shorter time it takes for the sample to be crystallized rapidly. Therefore, the connectivity of bcc-like clusters in samples may be responsible for the observed large scatter of the onset time of crystallization in undercooled liquid region as shown in Fig. 2(b). The difference of connectivity in different samples might result from the difference in the statistical distribution of local structures in high temperature liquids of metallic alloys. As high temperature liquid samples are quenching independently, glassy

samples with quite different local structures are obtained, where the connectivity of a type of local structures is different.

#### IV. CONCLUSION

In summary, in undercooled liquids of  $\text{Zr}_{85}\text{Cu}_{15}$  metallic glass-forming alloy, bcc-like crystal nuclei are formed during crystallization and responsible for the crystallization. The systematic analysis for the evolution of the bcc-like crystal nuclei reveals that as the stable critical crystal nucleus is forming, a strong spatial correlation is developing among the bcc-like crystal nuclei, which facilitate the subsequent rapid crystallization. A self-organized fractal feature of the crystal template has been revealed, and the rapid crystallization can be understood as the critical transition phenomenon. We show that the connectivity of bcc-like clusters in samples analyzed in terms of graph theory may be the structural origin of the observed large scatter of the onset of crystallization. Our findings may provide new perspectives on the structural origin and atomistic mechanism of the nucleation and growth of crystals in metallic glass-forming alloys as well as the nature of glass transition.

#### ACKNOWLEDGMENTS

This work was supported by the NSF of China (Grant Nos. 10972010, 51071174, 51271197, 50921091, and 11028206), NCET, and the Fundamental Research Funds for the Central Universities, and the Research Funds of Renmin University of China (Grant No. 10XNJ002).

<sup>1</sup>*Solidification and Crystallization*, edited by D. M. Herlach (Wiley VCH, 2004).

<sup>2</sup>R. Busch, J. Schroers, and W. H. Wang, *MRS Bull.* **32**, 620 (2007).

<sup>3</sup>W. L. Johnson, G. Kaltenboeck, M. D. Demetriou, J. P. Schramm, X. Liu, K. Samwer, C. P. Kim, and D. C. Hofmann, *Science* **332**, 828 (2011).

<sup>4</sup>H. W. Kui, A. L. Greer, and D. Turnbull, *Appl. Phys. Lett.* **45**, 615 (1984).

<sup>5</sup>Y. J. Kim, R. Busch, W. L. Johnson, A. J. Rulison, and W. K. Rhim, *Appl. Phys. Lett.* **65**, 2136 (1994); **68**, 1057 (1996).

<sup>6</sup>X. H. Lin, W. L. Johnson, and W. K. Rhim, *Mater. Trans., JIM* **38**, 473 (1997).

<sup>7</sup>W. H. Wang, *Prog. Mater. Sci.* **52**, 540 (2007).

<sup>8</sup>A. Masuhr, T. A. Waniuk, R. Busch, and W. L. Johnson, *Phys. Rev. Lett.* **82**, 2290 (1999).

<sup>9</sup>J. Schroers, W. L. Johnson, and R. Busch, *Appl. Phys. Lett.* **76**, 2343 (2000).

<sup>10</sup>J. Schroers, Y. Wu, R. Busch, and W. L. Johnson, *Acta Mater.* **49**, 2773 (2001).

<sup>11</sup>H. Assadi and J. Schroers, *Acta Mater.* **50**, 89 (2002).

<sup>12</sup>J. Z. Jiang, C. H. Jensen, and A. R. Rasmussen, *J. Metastable Nanocryst. Mater.* **15–16**, 81 (2003).

<sup>13</sup>Q. Wang, C. T. Liu, Y. Yang, Y. D. Dong, and J. Lu, *Phys. Rev. Lett.* **106**, 215505 (2011).

<sup>14</sup>J. Bokeloh, R. E. Rozas, J. Horbach, and G. Wilde, *Phys. Rev. Lett.* **107**, 145701 (2011).

<sup>15</sup>H. B. Yu, X. Shen, Z. Wang, L. Gu, W. H. Wang, and H. Y. Bai, *Phys. Rev. Lett.* **108**, 015504 (2012).

<sup>16</sup>T. Kawasaki and H. Tanaka, *Proc. Natl. Acad. Sci. U.S.A.* **107**, 14036 (2010); *Nature Commun.* **3**, 974 (2012).

<sup>17</sup>Y. Li, S. J. Poon, G. J. Shiflet, J. Xu, D. H. Kim, and J. F. Löffler, *MRS Bull.* **32**, 624 (2007).

<sup>18</sup>See <http://lammps.sandia.gov> for LAMMPS package.

<sup>19</sup>M. I. Mendeleev, D. J. Sordet, and M. J. Kramer, *J. Appl. Phys.* **102**, 043501 (2007).

<sup>20</sup>W. C. Swope and H. C. Andersen, *Phys. Rev. B* **41**, 7042 (1990).

<sup>21</sup>J. L. Finney, *Proc. R. Soc. London, Ser. A* **319**, 479 (1970).

<sup>22</sup>H. W. Sheng, W. K. Luo, F. M. Alamgir, J. M. Bai, and E. Ma, *Nature (London)* **439**, 419 (2006).

<sup>23</sup>M. Z. Li, C. Z. Wang, S. G. Hao, M. J. Kramer, and K. M. Ho, *Phys. Rev. B* **80**, 184201 (2009).

<sup>24</sup>H. L. Peng, M. Z. Li, and W. H. Wang, *Phys. Rev. Lett.* **106**, 135503 (2011).

<sup>25</sup>Y. Q. Cheng and E. Ma, *Prog. Mater. Sci.* **56**, 379 (2011).

<sup>26</sup>M. E. J. Newman, *SIAM Rev.* **45**, 167 (2003); *Proc. Natl. Acad. Sci. U.S.A.* **98**, 404 (2001).

<sup>27</sup>R. Albert and A.-L. Barabasi, *Rev. Mod. Phys.* **74**, 47 (2002).

<sup>28</sup>U. Gasser, E. R. Weeks, A. Schofield, P. N. Pusey, and D. A. Weitz, *Science* **292**, 258 (2001).

<sup>29</sup>A. Panaitescu, K. Reddy, and A. Kudrolli, *Phys. Rev. Lett.* **108**, 108001 (2012).

<sup>30</sup>P. Bak, C. Tang, and K. Wiesenfeld, *Phys. Rev. Lett.* **59**, 381 (1987); *Phys. Rev. A* **38**, 364 (1988).

<sup>31</sup>B. A. Sun, H. B. Yu, W. Jiao, H. Y. Bai, D. Q. Zhao, and W. H. Wang, *Phys. Rev. Lett.* **105**, 035501 (2010).

<sup>32</sup>J. L. Ren, C. Chen, Z. Y. Liu, R. Li, and G. Wang, *Phys. Rev. B* **86**, 134303 (2012).

<sup>33</sup>D. Ma, A. D. Stoica, and X.-L. Wang, *Nature Mater.* **8**, 30 (2009).

<sup>34</sup>T. Freltoft, J. K. Kjems, and S. K. Sinha, *Phys. Rev. B* **33**, 269 (1986).